Supplementary Material for the manuscript:

Large B-cell lymphoma imprints dysfunctional immune phenotype that persists years after treatment

Richard Pelzl[1,2,3,*], Giulia Benintende[1,2,3,*], Franziska Gsottberger[1,2,3], Julia K. Scholz[1,2,3], Matthias Rübner[2,4,5,6], Hao Yao[1,2,3], Kerstin Wendland[1,2,3], Kai Rejeski[2,7,8], Heidi Altmann[9], Srdjan Petkovic[1,2,3], Lisa Mellenthin[1,2,3], Sabrina Kübel[10], Moritz Schmiedeberg[10], Paulina Klein[10], Agnese Petrera[11], Rebecca Baur[1,2,3], Sophie Eckstein[2,4,5,6], Sandra Hoepffner-Grundy[12], Christoph Röllig[9], Marion Subklewe[2,4,13], Hanna Huebner[2,4,5,6], Georg Schett[3,14], Andreas Mackensen[1,2,3], Luca Laurenti[15], Frederik Graw[1,2,3], Simon Völkl[1,2,3,*], Krystelle Nganou-Makamdop[3,9,14,*], Fabian Müller[1,2,3,*]

Supplementary Material

Supplementary Table S1 Patient characteristics of the BC cohort

	Healthy Control (HC) (n=37)	Complete Remission (CR) after BC (n=30)	Newly Diagnosed (ND) BC (n=32)	p-values*
Sex				
Male n (%)	0	0	0	p = 0.99
Female n (%)	37 (100%)	30 (100%)	32 (100%)	
Median Age (CI)	62.1 [53.7 – 84.9]	65.3 [43.3 – 83.2]	67.5 [36.5 – 86.3]	p = 0.85
Disease Type				
Luminal A		6 (20%)	6 (19%)	p = 0.97
Luminal B		15 (50%	18 (56%)	
HER2+		2 (7%)	1 (3%)	
Basal-Like		4 (13%)	5 (16%)	
No Data		3 (10%)	2 (6%)	
UICC Stage				
Stage I		17 (57%)		
Stage II		10 (33%)		
Stage III		3 (10%)		
Stage IV		0		
No Data		0		
Treatment				
Surgery		30 (100%)		
Neoadj. CTx		9 (30%)		
Adj. CTx		2 (7%)		
Radiation		18 (60%)		
Antibody-based Tx		2 (7%)		
Hormone Tx		16 (53%)		
No Data		0		

Supplementary Table S2 Patient characteristics of the CLL cohort in watch & wait

	Healthy Control (HC) (n=33)	Active CLL (w&w) (n=35)	p-values*
Sex Male n (%) Female n (%)	 23 (70%) 10 (30%)	 26 (74%) 9 (26%)	p = 0.79
Median Age (CI)	63.5 [58.2 – 94.2]	71.8 [40.6 – 86.3]	p = 0.10
Binet Stage Binet A Binet B Binet C No Data		 24 (69%) 6 (17%) 4 (11%) 1 (3%)	
Median Lymphocytosis	2,232/µl [658 – 5,717]	16,155/µl [550 – 177,401]	**p = 0.0003**

Supplementary Table S3 Patient characteristics of the AML cohort

	Healthy Control (HC) (n=33)	AML (n=26)	p-values*
Sex			
Male n (%)	16 (62%)	16 (62%)	p = 0.99
Female n (%)	10 (38%)	10 (38%)	
Median Age (CI)	59.2 [40.0 – 69.1]	57.5 [24.0 – 75.0]	p = 0.73
Median Time from First Diagnosis to Second Sample (median [range])		16.1 [4.3 – 87.2]	
Disease			
De novo AML		26 (100%)	
AML-MR		0	
Cytogenetics			
Normal		18 (69%)	
inv(16)(p13q22)		6 (23%)	
t(8;21)(q22;q22)		1 (4%)	
del(13)(q12q14)		1 (4%)	
Trisomy 8		1 (4%)	
Trisomy 4		1 (4%)	
Molecular Genetics			
CEBPA		1 (4%)	
FLT3 ITD		6 (23%)	
FLT3 TKD		3 (12%)	
IDH1		0	
IDH2		4 (15%)	
NPM1		15 (58%)	
RUNX1		0	
TP53		0	

Abbreviations as: AML-MR=Acute myeloid leukemia with myelodysplasia-related changes

Supplementary Figure S1.

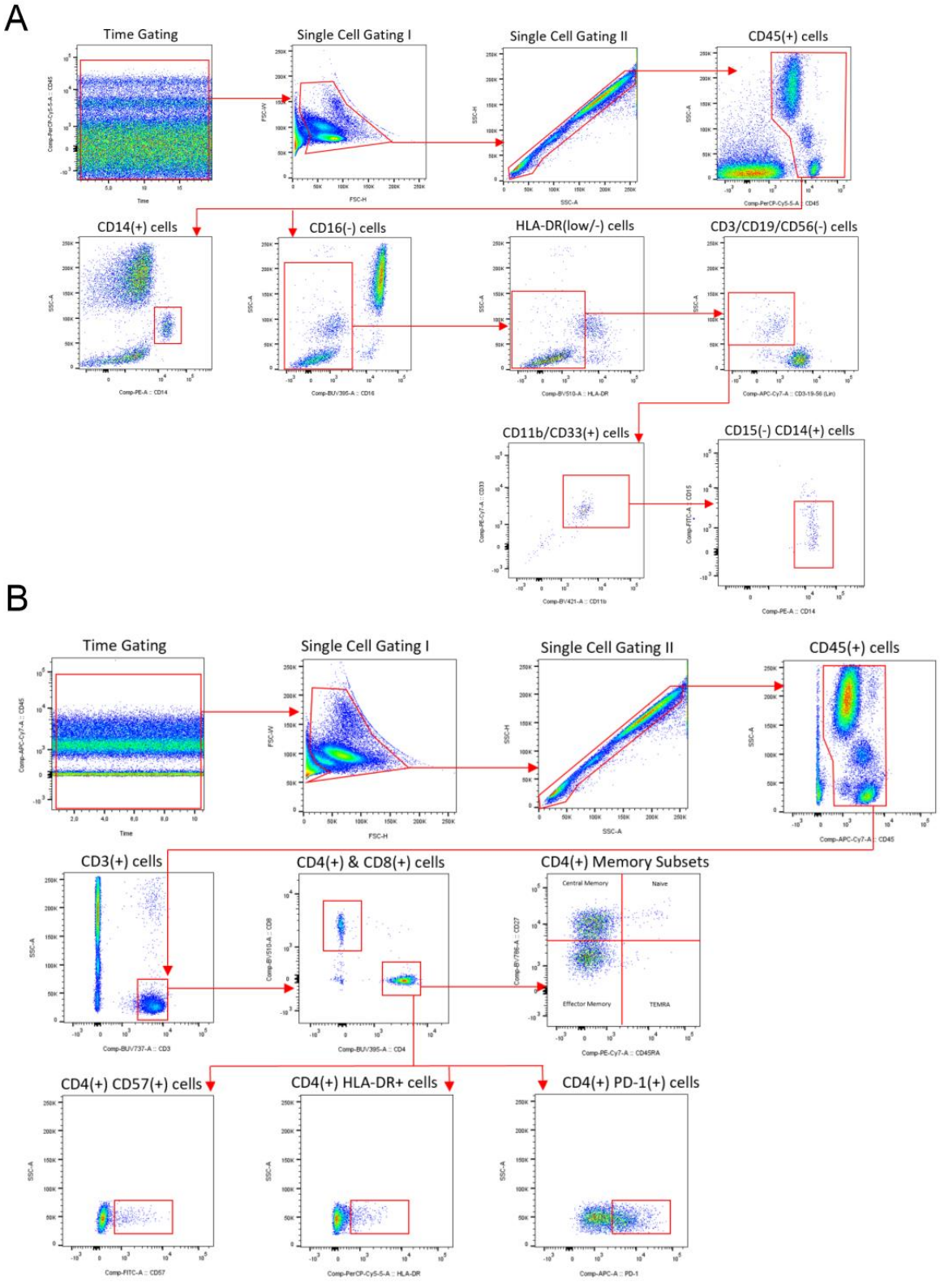

Representative dot plots of myeloid (A) and T cell (B) gating.

Supplementary Figure S2.

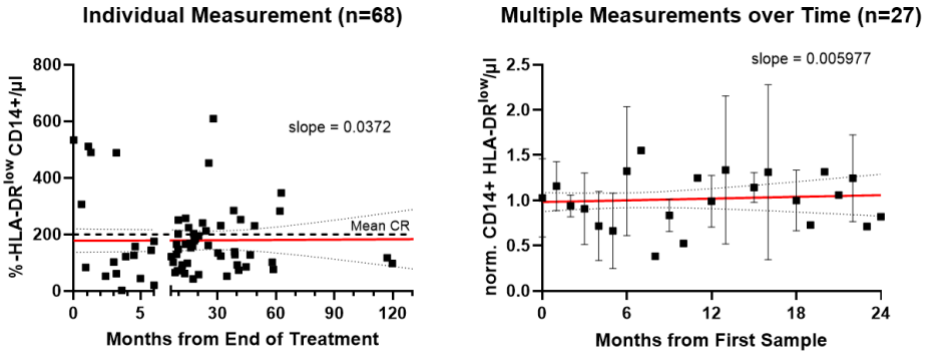

Absolute numbers of MDSCs do not change over time. Time point of individual CD14+/HLA-DR^{low} monocytes shown in A. In addition, 27 patients were measured longitudinally and normalized to the first measurement. The red lines indicate linear regression over time including 95%-CI and slope.

Supplementary Figure S3.

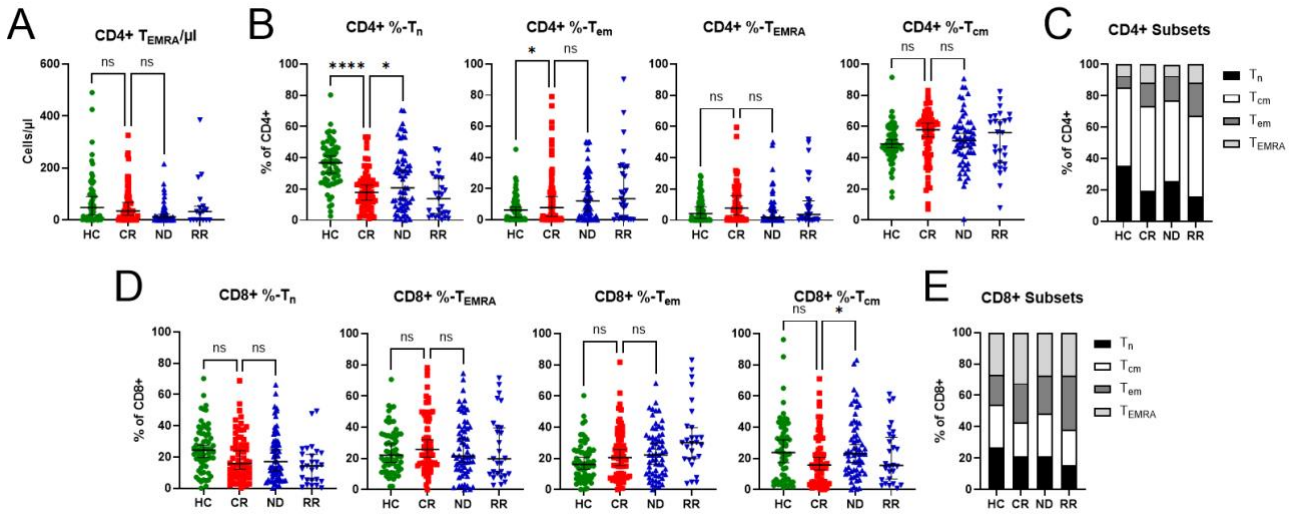

Phenotype of the remaining T-cell subsets not shown in the main article as determined by flow cytometry. (A) The absolute count of CD4+ T_{EMRA} cells is not significantly altered in DLBCL patients in complete remission (CR). HC=healthy control, CR=complete remission after DLBCl, ND=newly diagnosed DLBCL, RR=relapsed/refractory DLBCL. (B) The indicated CD4+ T-cell subsets are altered in different disease stages. (C) The relative fraction of T_n decreases in CR while T_{em} and T_{EMRA} expand. (D) The indicated CD8+ T-cell subsets change less substantially than CD4+ subsets. (E) In CD8+ T-cells not only T_n but also T_{cm} decrease whereas T^{em} and T_{EMRA} increase in fraction. For all figures each symbol represents an individual patient, p-values were determined by ANOVA as ns=not significant, *p<0.05, **p<0.01, ***p<0.001, ***p<0.0001.

Supplementary Figure S4.

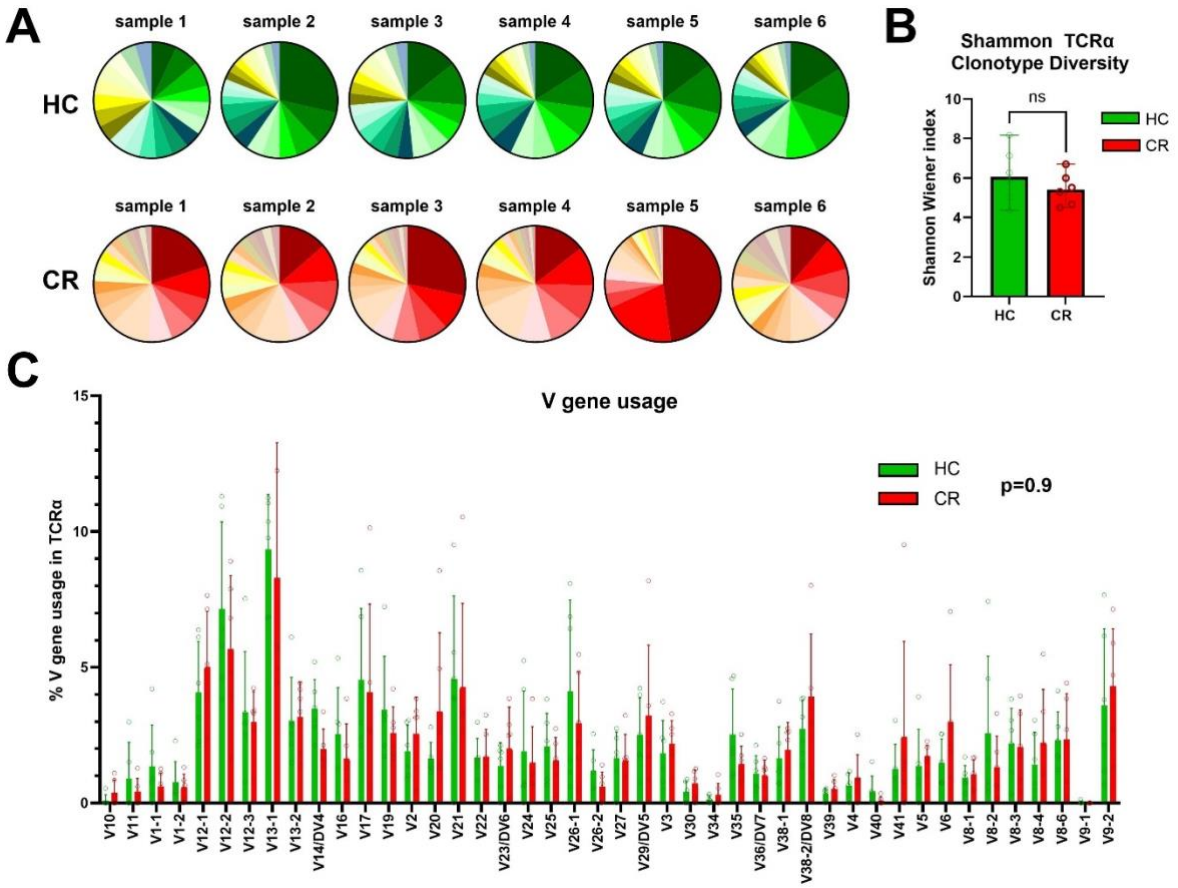

TCR sequencing comparing TEMRA population of HC and patients in CR. TCR sequencing shows that the top 20 clonotypes were similar in size and distribution between HC and CR, and so was the TCR diversity determined by Shannon. The V-gene usage was comparable between the two groups and polyclonal, suggesting no mono- or oligoclonal expansion or reduced diversity in the CR patients.

Supplementary Figure S5.

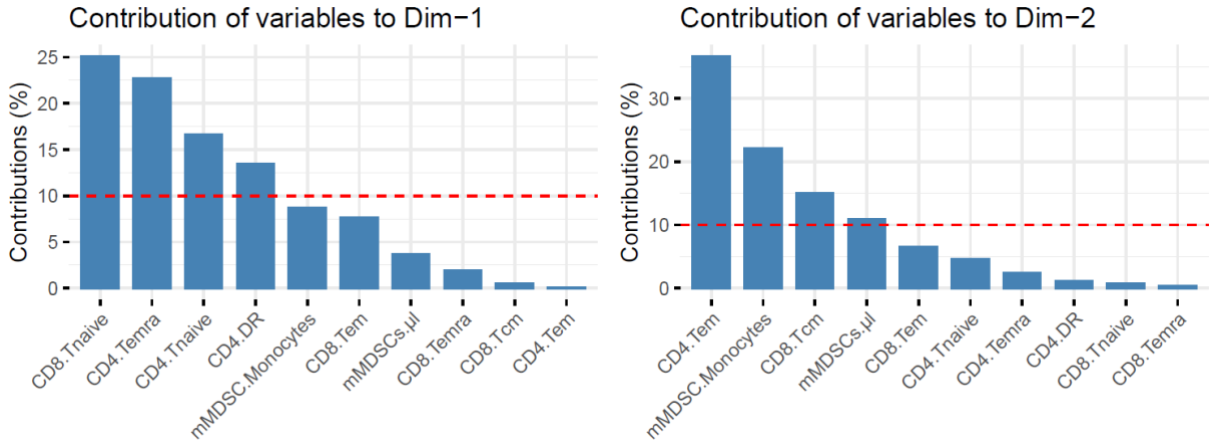

Relative contribution of the individual variables that defined dimension 1 and 2 of the principal component analysis, i.e., the first two principal components, within Figure 2H.

Supplementary Figure S6.

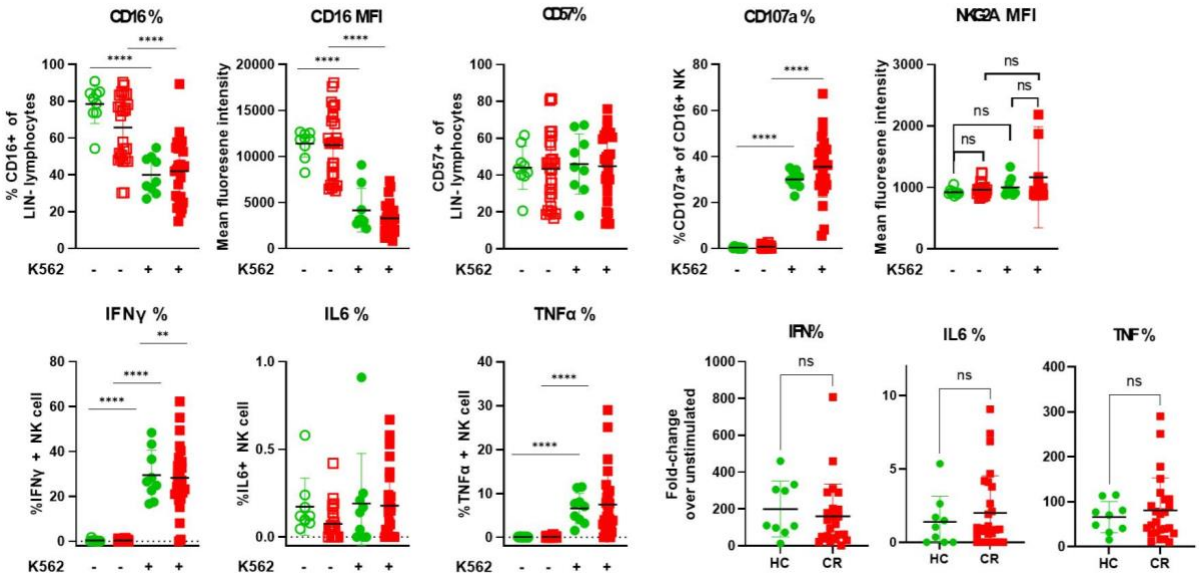

NK cell phenotype and activation. Representative NK cells of HC (n=9, green) and of patients in CR (n=23, red) were stained for NK cell markers. Dump neg. cells were analyzed for CD16, CD57, degranulation marker CD107a, and expression level of NKG2A at base-line and after 24h of activation by HLA-type I negative K562. Intracellular levels of IFNγ, IL6, and TNFα at baseline and after activation were determined and fold-change after activation within each matched sample pair determined. Each symbol represents an individual person. Significance determined by T-tests. If no significance is indicated, difference was not significant ($p>0.05$).

Supplementary Figure S7.

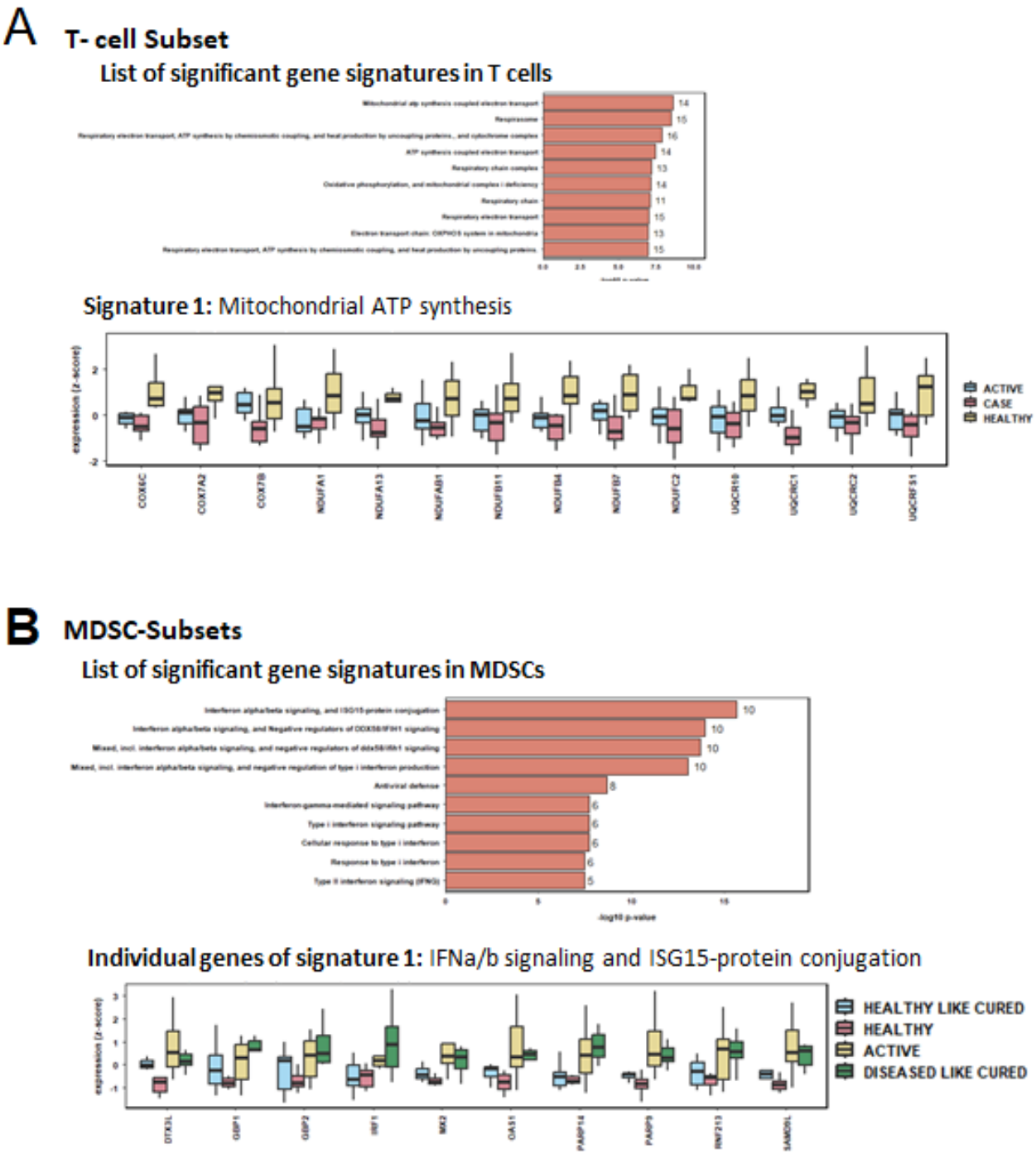

Extended data of the pathway analysis of the RNA bulk sequencing. (**A**) Genes involved in signature three of activated (HLA-DR+) T-cells. (**B**) Genes involved in signature three of CD14+ HLA-DR^{low} monocytes.

Supplementary Figure S8.

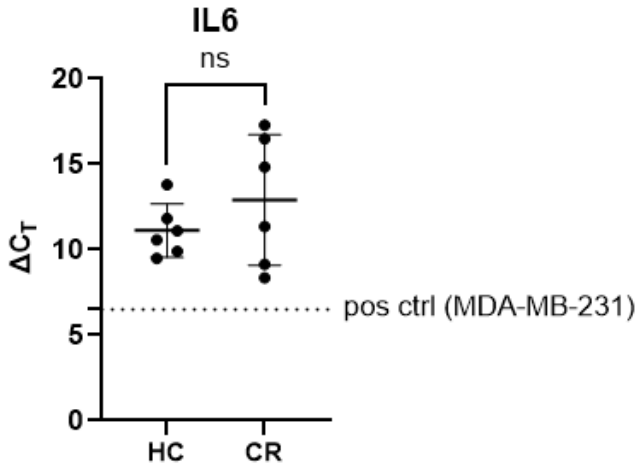

mRNA level of IL6 in MDSCs of patients in remission compared with healthy control. mRNA levels of IL6 and GAPDH (house-keeping gene) were analyzed by one-step RT-qPCR. Relative to house-keeping gene cycle number (=0), the IL6-expressing positive control MDA-MB-231 (BC cell line) appeared at much lower cycles compared with IL6 real-time signals of MDSCs of healthy donors (HC) compared with patients in complete remission (CR). Each symbol represents a patient. All reactions were performed in technical duplicates. Significance was determined by unpaired T-test to ns=not significant.

Supplementary Figure S9.

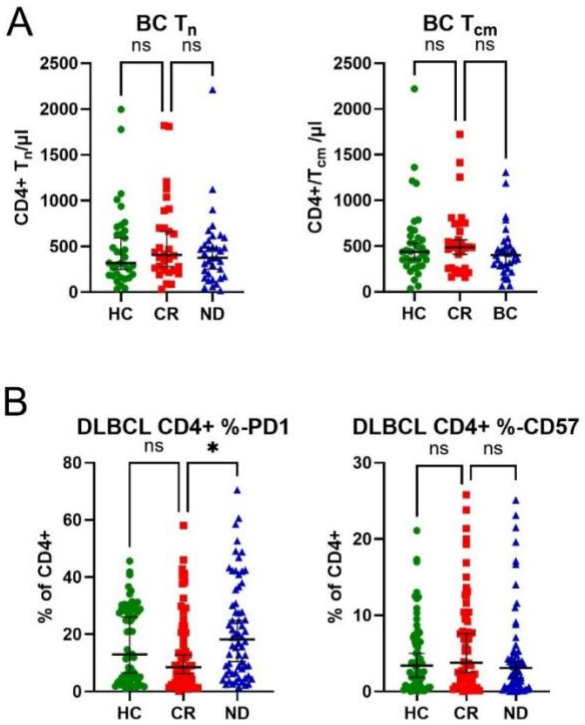

(A) Absolut numbers of indicated T-cell subsets in healthy controls (HC), in newly diagnosed (ND) breast cancer and in breast cancer patients in complete remission (CR). (B) CR DLBCL patients do not show higher exhaustion or senescence in CD4+ T cells compared to HC. Each symbol represents an individual patient. Significance was determined by ordinary one-way ANOVA as ns = not significant.

Supplementary Figure S10.

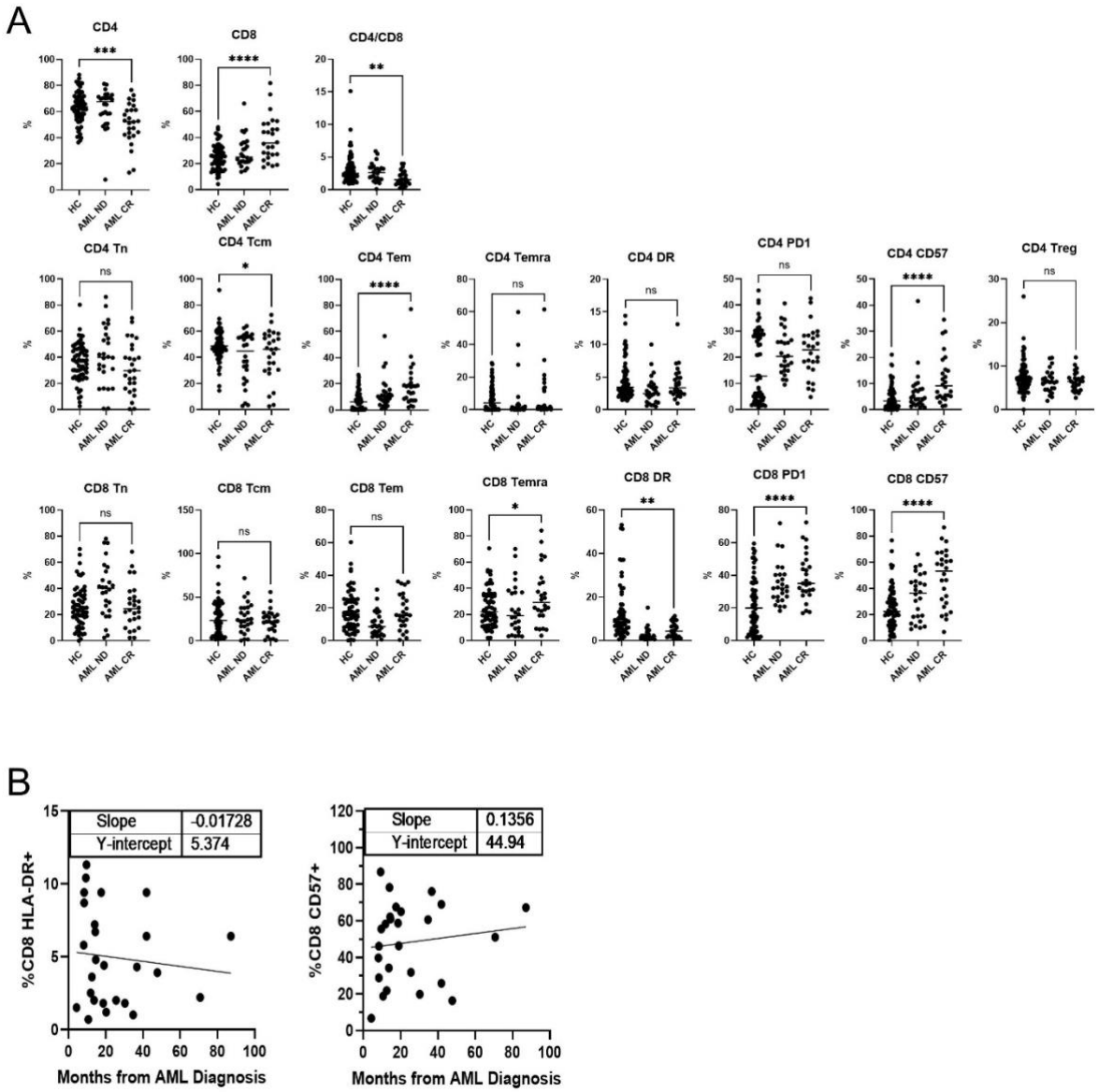

T cell phenotype of patients with AML at first diagnosis compared with last banked follow up sample. (A) CD4 and CD8 t cell subsets analyzed from thawed PBMC samples of patients with first diagnosis of AML and at their last follow-up while still in CR. Patient characteristics are summarized in suppl. table S4. Each dot indicates an individual patient when newly diagnosed (ND) or their paired sample at the last known follow-up (CR). Healthy control (HC) samples were statistically compared with CR using unpaired T test with p>0.05=ns, p<0.05=*, p<0.01=**, p<0.001=***, and p<0.0001=****. (**B**) Simple linear regression analysis of indicated sample parameters and respective sampling time point relatively to first diagnosis.

Supplementary Figure S11.

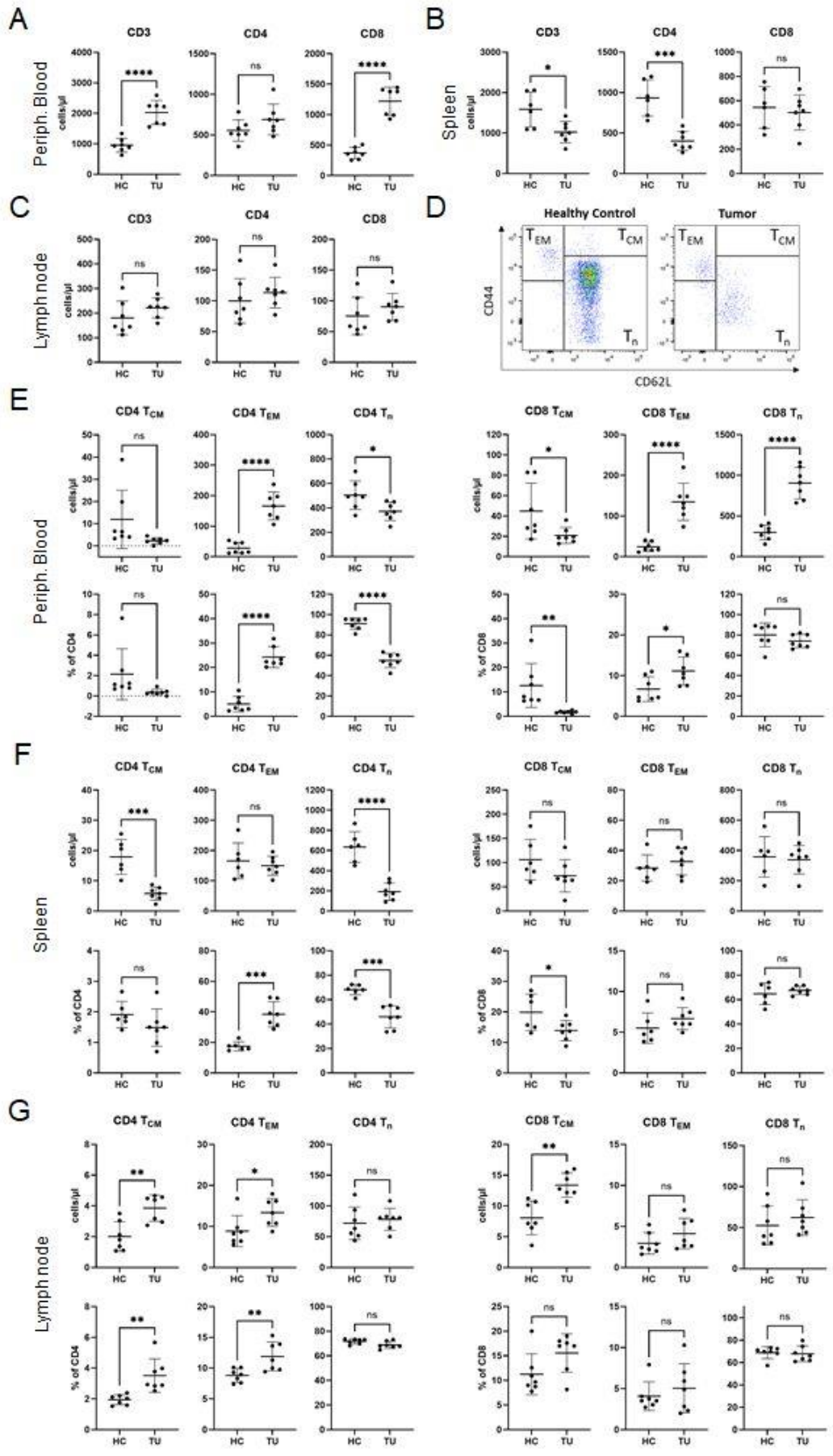

Suppl. Fig. S9. Mouse T cell changes upon B-NHL growth. Thirty-eight days after i.v. injection of syngeneic B-NHL cells, peripheral blood (A), spleen (B), and lymph nodes (C) show indicated changes in T cells/µl; shown are CD3, CD4, and CD8. Numbers were generated using counting beads, HC = healthy mouse control, TU = tumor-bearing mice; each symbol represents measurements of one individual mouse, n = 5 mice per group, significance determined by unpaired T-test. (**D**) show the gating strategy and nomenclature for the now following T cell subclass phenotyping. (**E-G**) T_n, T_{cm}, and T_{em} for CD4 (left panel) and for CD8 (right panel) in absolute numbers (top panel) and % (bottom panel) for peripheral blood (E), spleen (F), and lymph nodes (G). Numbers, symbols and statistics are as defined in (A).

Supplementary Material and Methods

Patients

Patients with newly diagnosed histologically confirmed DLBCL, BC or chronic lymphocytic leukemia (CLL) as well as patients in CR were enrolled only if they had no history of other malignant tumors, chronic infections or autoimmune diseases. Patients with primary central nervous system lymphoma or primary mediastinal B-cell lymphoma were excluded. BC and DLBCL patients were considered to be in CR based on CT or PET/CT scans performed after the last cycle of chemotherapy, immunotherapy, hormone therapy or surgery, respectively. They were enrolled the earliest at the first follow-up appointment three months after concluding therapy. Patients with BC were categorized by their molecular subtype and staged according to the UICC guidelines (**Supplementary table S1**). Patients with active CLL in watch and wait (w&w) were staged according to Binet (**Supplementary table S2**). As control group, healthy controls (HC) with no previous history of malignant, chronic infectious, or autoimmune diseases were recruited.

Sample preparation, antibodies, and flow cytometry

Fresh whole blood, if not otherwise indicated, was stained within 1 to 4 hours after sample acquisition and measured by flow cytometry. PBMCs were isolated from EDTA blood tubes by centrifugation over a Pancoll layer (Pan Biotech, Aidenbach, Germany) of 1.077 g/mL density. Monoclonal antibodies (mAbs) were purchased from BD Biosciences and Biolegend. Whole blood was stained according to manufacturer´s recommendations using FACS Lysing Solution (BD Biosciences) and fluorochrome-coupled antibodies as listed in supplements. Total cell counts were determined using TruCount Tubes (BD Biosciences). For intracellular staining cells were fixed and permeabilized using Perm/Wash Buffer (BD Biosciences) in line with manufacturer´s instructions. Measurements were recorded and analyzed using a FACS Fortessa flow cytometer (BD Biosciences) and FlowJo, version 9.0.2. software (TreeStar, San Carlos, CA).

T-cell Proliferation Assay

A MoFlo XDP (Beckman Coulter, USA) was used to flow sort myeloid cells and autologous T-cells (CD3+). M-MDSCs were defined as Lineage (Lin)- CD16- CD11b+ CD14+ HLA-DR$^{-/low}$. Myeloid controls were defined as Lin- CD16- CD11b+ CD14+ HLA-DR^{high}. The purity of sorted cells was >95%. T-cells were incubated with CFSE (5 µM, Invitrogen, USA). Next, M-MDSCs and CD14+HLA-DR+cells were cocultured with CFSE-labeled T-cells, respectively, in a 96-well plate at the ratio of 1:1 and 1:2. All cells were cultured with anti-CD2, anti-CD3, anti-CD28 at 1:2 ratio (Miltenyi Biotec, Bergisch Gladbach). The suppressive ability of M-MDSCs on T-cells was analyzed by flow cytometry 7 days later.

T-cell Stimulation Assay

Cryopreserved PBMCs of patients and HC were cocultured with SARS-Cov2 Spike peptides obtained through BEI Resources, NIAID, NIH: Peptide Array, SARS-related Coronavirus 2 Spike (S) Glycoprotein, NR-52402. Two hours after addition of antigens, 2 µM Monensin (Biolegend) was added for overnight stimulation. Next, cells were stained with surface and intracellular antibodies, detailed in the supplements. Stained cells were acquired on an AttuneNxt (Thermofisher). For measurement of IFN-γ- concentrations in culture supernatants, PBMCs were stimulated with Spike peptide pool as described above and incubated for 3 days. Collected supernatant was stored at -20°C until measurement by IFN-γ ELISA (R&D Systems) according to the manufacturer's instructions.

NK cell assays

Cryopreserved PBMCs from patients in CR and HC were thawed and cultured overnight in complete medium at 37°C. The following day, PBMCs were cocultured with K562 target cells at a 2:1 effector-to-target ratio for 4 hours at 37°C. Monensin (BioLegend, 2 µM), Brefeldin A (BioLegend, 5 µg/mL), and anti-CD107a antibody were added at the beginning of the incubation to allow detection of degranulation. After stimulation, cells were harvested and stained for surface markers (CD3, CD14, CD16, CD19, CD33, CD56, CD57, NKG2A), followed by fixation and intracellular staining for IL-6, IFN-γ, and TNF-α. Stained cells were subsequently acquired and analyzed by flow cytometry to assess NK cell activation and functional responses.

Cytokine measurements

Serum levels of IL-6, sCD25, CXCL9, CXCL10 and β2-micorglobulin were determined using ELISA kits (R&D Systems, Minneapolis, MN). Serum proteomic analysis with an expanded set of immunomodulatory cytokines was quantified as part of the Olink®Target 96 Immuno-Oncology Panel by proximity extension technique (Olink, Uppsala, Sweden) as previously described in detail [26,27].

IL-6 Monocyte Stimulation Assay

Monocytes were isolated from PBMCs of healthy donors by plastic adhesion, plated in RPMI-1640 medium with GM-CSF (50 ng/ml), with or without IL-6 (20 or 50 ng/ml) and incubated for 6 days. Samples were analyzed by flow cytometry, defining MDSCs as CD14+ CD11b+ HLA-DR^{low} cells.

Animal model

For systemic tumor growth C57BL/6 mice were injected with one million B-cell lymphoma cells, carrying a λ-*myc* translocation in the tail vein as previously described [29]. On day 38 after tumor injection mice were humanely sacrificed. Blood was drawn from the heart *post mortem*. Single

cell suspensions of LN and spleen were prepared by meshing organs through a 70 µm cell strainer. The staining for flow cytometry was performed as described above.

Real-Time PCR

Total RNA was extracted from sorted MDSCs of healthy donors and patients in complete remission (as described previously) using the RNeasy Mini Kit (Qiagen). The breast cancer cell line MDA-MB-231, which is known to express IL6, served as positive control. cDNA synthesis and quantitative real-time (RT-qPCR) were performed using the Luna® Universal One-Step RT-qPCR Kit (New England Biolabs) and the Rotor-Gene Q cycler (Qiagen). Gene-specific primers were ordered from Qiagen (IL6: #QT00083720, GAPDH: #QT00079247). All reactions were performed in technical duplicates.

RNA sequencing

A MoFlo XDP (Beckman Coulter, USA) was used to flow sort HLA-DR^{low} monocytes (CD14+, HLA-DR^{low}) and activated CD4+ T-cells (CD4+, HLA-DR+) from freshly isolated PBMCs. RNA was extracted with RNeasy kit (Qiagen, USA), according to manufacturer´s protocol. The RNA was sequenced at Eurofins Genomics (Constance, Germany) using an INVIEW Transcriptome Discover product. This included purification of mRNA, fragmentation, strand-specific cDNA synthesis, end-repair, ligation of sequencing adapters, amplification and purification. The prepared libraries were then quality-checked, pooled and sequenced on an Illumina platform (Illumina NovaSeq6000, PE150 mode).

FastQ files were used as starting point for outlined biostatistical analyses. The multiple pairwise differential expression workflow was generated using Searchlight 2 (v2.0.3). Per sample group mean expression values and standard deviations per gene were calculated using numpy. Next the differential expression tables were combined with the expression set, to create the "differential expression set". A list of significantly differentially expressed genes was generated from the differential expression set using the adjusted p threshold of 0.05 and the absolute log2fold threshold of > 0.0. Finally, all plots were generated with ggplot2.

To generate the differential expression signatures firstly each gene was classified into a starting signature based on its pattern of significant differential expression over the comparisons. Genes that were unchanged in all differential comparisons were excluded. Next the values for each gene was converted into an expression z-score. For each signature a metagene expression value was created. To determine signatures with a similar expression profile, for each pairwise combination of signatures the two expression metagenes were correlated to each other using a Spearman Correlation Coefficient. Over Representation Analysis (ORA) was performed using the STRING11.5. To correct for multisampling a Benjamini-Hochberg correction was applied. Gene sets with an adjusted p-value of 0.05 and an absolute log2fold enrichment above 0.0 were considered significant (Cole et al. 2021).

TCR Sequencing

A MoFlo XDP (Beckman Coulter, USA) was used to sort activated HLA-DR+ CD4+ T-cells (CD4+, HLA-DR+). RNA was extracted with RNeasy kit (Qiagen, USA), according to manufacturer´s protocol. The library for targeted NGS sequencing of human T-cell receptor (TCR) was prepared by QIAseq Targeted RNA Panel TCR Library Kit (Qiagen, USA), according to manufacturer´s protocol. The prepared libraries were sequenced at paired-end, 600 cycles on Illumina NextSeq at the local NGS Core facility. Data analysis was performed on the web-based GeneGlobe platform (Qiagen, USA), which generates clonotype calls using the IMSEQ software [28].

Multivariate analysis

A principal component analysis (PCA) was performed to identify immunophenotypic patterns among all patients in complete remission (CR). Patients and variables were filtered subsequently to only consider (i) patients with less than 50% of variables missing, and (ii) only variables with having complete information for all remaining patients, leaving a set of 55 patients in CR and 10 variables considered within the PCA. Variables were selected based on univariate significant differences to either HC and/or AD. To compare individual CR profiles to HC and patients in RR, the immunophenotypes of HC and RR were mapped onto the PCA-mapping for CR by using the obtained PCA-model. Robustness of obtained patterns was examined by also considering additional variables within the PCA analysis, with missing values for individual patients being imputed using the regularized iterative PCA algorithm, which did not affect the presented results. Analysis was performed in R version 4.3.2 using function PCA of package *FactoMineR*.